Ultrasound Assessment of Inflammation and Renal Tissue Injury With Microbubbles Targeted to P-Selectin

Jonathan R. Lindner, MD; Ji Song, PhD; Jonathan Christiansen, MB, ChB; Alexander L. Klibanov, PhD; Fang Xu, MD; Klaus Ley, MD

Background—Routine methods capable of assessing tissue inflammation noninvasively are currently not available. We hypothesized that tissue retention of microbubbles targeted to the endothelial cell adhesion molecule P-selectin would provide a means to assess inflammation with ultrasound imaging.

Methods and Results—Phospholipid microbubbles targeted to P-selectin (MB_p) were created by conjugating monoclonal antibodies against murine P-selectin to the lipid shell. The microvascular behaviors of MB_p and control microbubbles without antibody (MB) or with isotype control antibody (MB_{iso}) were assessed by intravital microscopy of cremasteric venules of control and tumor necrosis factor (TNF)-α–stimulated wild-type mice. Retention of all microbubbles increased ($P<0.05$) with TNF-α treatment because of increased attachment to activated leukocytes. Extensive attachment of MB_p directly to the venular endothelium or to adherent platelet-leukocyte aggregates was observed in TNF-α–stimulated mice, resulting in 4-fold greater ($P<0.01$) retention of MB_p than either MB_{iso} or MB. Enhanced retention of MB_p was completely abolished in TNF-α–stimulated P-selectin–deficient mice. The ultrasound signal from microbubbles retained in inflamed tissue was assessed by contrast-enhanced renal ultrasound imaging of the kidneys of mice undergoing ischemia-reperfusion injury. In wild-type mice, this signal was significantly higher ($P<0.05$) for MB_p (12 ± 2 U) than either MB_{iso} (6 ± 3 U) or MB (5 ± 3 U). In P-selectin–deficient mice, the signal for MB_p was equivalent to that from control microbubbles.

Conclusions—Microvascular retention of microbubbles targeted to P-selectin produces strong signal enhancement on ultrasound imaging of inflamed tissue. These results suggest that site-targeted microbubbles may be used to assess inflammation, tissue injury, and other endothelial responses noninvasively with ultrasound. **(*Circulation*. 2001;104: 2107-2112.)**

Key Words: contrast media ■ cell adhesion molecules ■ echocardiography ■ inflammation

We recently demonstrated that tissue inflammation can be assessed noninvasively by ultrasound imaging of microbubbles that are retained by activated leukocytes.[1,2] Albumin and lipid microbubbles attach to leukocytes adherent to the venular endothelium and are phagocytosed intact within minutes.[1–3] The ultrasound signal from these microbubbles, however, is relatively low because of the small proportion of microbubbles that are retained and viscoelastic damping of microbubbles once phagocytosed.[1] This signal has been enhanced by incorporation of specific lipid moieties in the microbubble shell that enhance microbubble avidity for activated leukocytes.[2]

A more direct method for assessing microvascular inflammatory responses is possible by conjugating ligands for specific endothelial cell adhesion molecules to the microbubble shell.[4] Potential advantages of this strategy include a greater number of retained microbubbles, less acoustic damping (because they remain extracellular), and the ability to quantify expression of specific adhesion molecules.

In the present study, we developed lipid microbubbles bearing antibodies against P-selectin, an endothelial cell adhesion molecule expressed during inflammatory responses[5] and ischemia-reperfusion.[6] We hypothesized that abundant retention of targeted microbubbles in inflamed tissue would result in a strong ultrasound signal and provide a means to image early inflammatory responses by use of intravenous administration of microbubbles. These hypotheses were tested by evaluating the microvascular behavior of targeted microbubbles in wild-type and P-selectin–deficient ($P^{-/-}$) mice with intravital microscopy and by performing contrast-enhanced renal ultrasound early after ischemia-reperfusion injury.

Methods

Preparation of Microbubbles

Control lipid microbubbles (MB) and microbubbles with monoclonal antibodies against P-selectin (MB_p) or isotype control antibodies (MB_{iso}) conjugated to their surfaces were created. Biotinylated

Received May 28, 2001; revision received July 18, 2001; accepted July 19, 2001.

From the Cardiovascular Division (J.R.L., J.S., J.C., F.X.) and the Department of Biomedical Engineering (J.S., K.L.), University of Virginia School of Medicine, Charlottesville, and Mallinckrodt Medical, Inc, St Louis, Mo (A.L.K.).

Correspondence to Jonathan R. Lindner, MD, Box 158, Cardiovascular Division, University of Virginia Medical Center, Charlottesville, VA 22908. E-mail jlindner@virginia.edu

Circulation **is available at http://www.circulationaha.org**

microbubbles containing decafluorobutane gas were prepared as previously described.[7] Approximately 3×10^8 biotinylated microbubbles were incubated for 30 minutes with 90 μg streptavidin (Sigma) and washed. Aliquots of the suspension (1×10^8 microbubbles) were incubated for 30 minutes with 75 μg of biotinylated (EZ-Link, Pierce) rat anti-mouse monoclonal IgG1 against P-selectin (RB40.34) or isotype control antibody (R3-34, Pharmingen Inc). The antibody concentration used was determined by flow cytometry experiments (below).

Flow Cytometry

Flow cytometry was used to determine the antibody concentration needed for binding-site saturation. Biotinylated microbubbles (1×10^8) were incubated as above with streptavidin, then 0.75 to 750 μg of FITC-labeled biotinylated R3-34. Microbubbles (1×10^5 events) were analyzed on a FACSCalibur (Becton Dickinson) to generate histograms of green fluorescence intensity.

Animal Preparation

The study protocol was approved by the Animal Research Committee at the University of Virginia. Mice were anesthetized with an injection (12.5 μL/g IP) of a solution containing ketamine hydrochloride (10 mg/mL), xylazine (1 mg/mL), and atropine (0.02 mg/mL). Body temperature was maintained at 37°C with a heating pad. Both jugular veins were cannulated for administration of microbubbles and drugs.

Intravital Microscopy

Inflammation of the cremaster muscle was produced by intrascrotal injections of 0.5 μg murine tumor necrosis factor (TNF)-α (Sigma) 2 hours before surgery in 5 wild-type mice and in 5 $P^{-/-}$ mice obtained from established colonies derived from a gene-targeted founder.[8] Five untreated wild-type mice served as controls. A cremaster muscle was prepared as previously described[3] and was superfused continuously with isothermic bicarbonate-buffered saline. Observations were made with an Axioskop2-FS microscope (Carl Zeiss, Inc) with a saline-immersion objective (SW 40/0.8 numerical aperture). Video recordings were made with a high-resolution CCD camera (C2400, Hamamatsu Photonics) interfaced with a video time-display unit (VTG-33, For-A Ltd) connected to an S-VHS recorder (S9500, JVC).

For microscopy, a fluorescent lipid probe (excitation wavelength ≈500 nm) was incorporated into the lipid shell.[2] Microscopy was performed with combined fluorescent epi-illumination (460- to 500-nm excitation filter) and low-intensity transillumination. Twenty optical fields encompassing 20- to 40-μm venules were recorded 4 minutes after injection of 5×10^6 MB, MB_{iso}, or MB_p microbubbles in random order to determine the number of microbubbles retained and to classify the mechanism of retention as either attachment to leukocytes, attachment to the endothelium, or indeterminate. In 2 of the TNF-α–treated wild-type mice, injections of MB_p were repeated after in vivo labeling of platelets with intravenous injection of 50 μL of 0.05% rhodamine-6G (Molecular Probes).[9] Microscopic observations were repeated with fluorescent epi-illumination with 530- to 560-nm and 460- to 500-nm excitation filters to ascertain the extent of microbubble interactions with activated platelets or leukocyte-platelet complexes.

Venular segments were recorded under transillumination at regular intervals. Centerline blood velocities were measured in these segments with a dual-slit photodiode (CircuSoft Instrumentation) and converted to mean blood velocities (V_b) by multiplying by 0.625.[10] Shear rates (γ_w) were determined by the equation $\gamma_w=2.12(8V_b)/d$, where d is the vessel diameter and 2.12 is a correction factor for the shape of the velocity profile.[11]

Determination of Leukocyte Adhesion and Rolling Fraction

Intravital microscopy video recordings were analyzed offline. The number of rolling leukocytes (r_n) was determined by counting leukocytes crossing a line perpendicular to the vessel in 1 minute. Leukocyte rolling flux fraction (F), which reflects the percentage of leukocytes in transit that are rolling, was calculated by the equation $F=r_n/(0.25\pi d^{2\times}V_{b\times}60\times C_L)$, where d is vessel diameter, V_b is centerline blood velocity, and C_L is the systemic blood leukocyte concentration.[12] The number of adhered leukocytes, defined as those stationary for >30 seconds, was expressed per venular surface area.

Contrast-Enhanced Renal Ultrasound

Five wild-type and 3 $P^{-/-}$ mice were anesthetized, and a kidney was exposed by dorsal paramedian opening of the retroperitoneal space.[13] A hemostatic microvascular clamp (B-1A, ASSI Corp) was placed on the renal pedicle for 30 minutes, then removed. The surgical wound was closed in layers.

Renal ultrasound was performed in the mice undergoing renal ischemia 1 hour after reflow and in 3 control (nonischemic) wild-type mice. Harmonic imaging (Sequoia, Acuson Corp) was performed at a transmission frequency of 2.5 MHz and a mechanical index of 1.9. Images were acquired with a water bath as an interface between the transducer and the dorsum. The acoustic focus was placed at the level of the renal pelvis, and gain settings were optimized and held constant. Data were recorded on 1.25-cm videotape with an S-VHS recorder (SVO-9500 MD, Sony).

Intravenous injections of 5×10^6 MB, MB_{iso}, and MB_p were made in random order, and ultrasound imaging was not initiated until 8 minutes after each injection to allow clearance of freely circulating microbubbles from the blood pool.[2] The video intensity (VI) in the initial frame was used to determine total tissue concentration of microbubbles within the ultrasound beam (retained and freely circulating).[1,2] These microbubbles were destroyed by 2 to 3 seconds of continuous imaging (>50 Hz), after which the ultrasound pulsing interval (PI) was increased to 10 seconds to allow complete replenishment of the beam with microbubbles[14] and derivation of signal from freely circulating microbubbles alone.[1,2] Several averaged precontrast frames were digitally subtracted from the initial contrast-enhanced frame and from several averaged frames obtained at a PI of 10 seconds. Background-subtracted VI was measured from a region of interest placed around each kidney.

Immunohistochemistry

Immunostaining for P-selectin was performed on paraffin-embedded sections of renal tissue. Affinity-purified rabbit polyclonal antibodies against the cytoplasmic domain of P-selectin[15] (kindly provided by Samuel Greene, PhD, University of Virginia) were used as a primary antibody, followed by a biotinylated goat anti-rabbit secondary antibody (Vector Laboratories). Staining was performed with a peroxidase kit (ABC Vectastain Elite, Vector Laboratories) and 3,3′-diaminobenzidine chromagen (Dako). Slides were counterstained with hematoxylin.

Statistical Methods

Data are expressed as mean±SD. Interval comparisons were made with repeated-measures ANOVA. Comparisons of nominal data were made with χ^2 analysis-of-contingency tables and Yates correction for continuity. Differences were considered significant at a value of $P<0.05$ (2-sided).

Results

Flow Cytometry

Conjugation of FITC-labeled antibodies to microbubbles was demonstrated by flow cytometry (Figure 1). Incubation of microbubbles with increasing concentrations of antibody resulted in incrementally greater microbubble fluorescent intensity until a saturation concentration of just over 7.5 μg of antibody per 1×10^8 microbubbles was reached (equivalent to an antibody:microbubble ratio of $[3\times10^5]$:1).

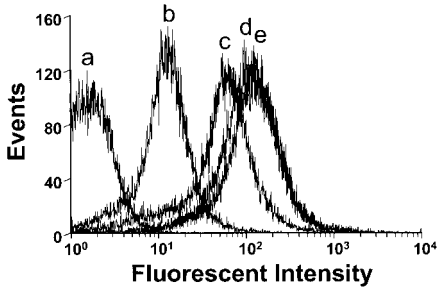

Figure 1. Antibody conjugation to surface of biotinylated microbubbles. Histograms of green fluorescence intensity obtained by flow cytometry of microbubbles after incubation with increasing concentrations of FITC-labeled biotinylated R3-34 (a, 0 μg; b, 0.75 μg; c, 7.5 μg; d, 75 μg; e, 750 μg antibody per 1×10^8 microbubbles) demonstrated increased binding until saturation was achieved (between 7.5 and 75 μg per 1×10^8 microbubbles).

Characterization of Microbubble Retention

The mean blood flow velocity and shear rate in the cremaster venules did not differ between groups (Table). As previously described,[12] TNF-α stimulation in wild-type animals did not affect leukocyte flux fraction but did increase leukocyte adhesion several-fold (Table). Compared with TNF-α–treated wild-type mice, treated $P^{-/-}$ mice possessed a much lower rolling flux fraction, whereas leukocyte adhesion was minimally reduced (Table).

In the cremaster venules of untreated wild-type mice, retention of MB_p was slightly greater than that of MB or MB_{iso} (Figure 2). TNF-α treatment in wild-type mice resulted in a significant increase in retention for all of the microbubble agents, the extent of which was much greater for MB_p than control microbubbles (MB_{iso} and MB) (Figure 2). In these animals, retention was greater for MB_{iso} than for MB. Enhanced retention of MB_p after TNF-α stimulation was completely abolished in $P^{-/-}$ mice (Figure 2).

Greater retention of MB_p than control microbubbles in untreated and TNF-α–treated wild-type mice was largely a result of direct microbubble attachment to the endothelium, which did not occur with the control microbubbles (Figure 3). In TNF-α–treated wild-type mice, the mechanism for MB_p attachment was also frequently classified as indeterminate. Enhanced retention of MB_p in response to TNF-α was abolished in $P^{-/-}$ mice because of the absence of endothelial and indeterminate attachment of microbubbles (Figure 3).

Venular Hemodynamic Parameters and Leukocyte Rolling and Adhesion Data

	Wild-Type (Untreated)	Wild-Type+ TNF-α	$P^{-/-}$+ TNF-α
Venular diameter, μm	28±6	29±5	30±4
Blood velocity, μm/s	2055±739	2442±1001	1864±342
Wall shear rate, s^{-1}	1251±391	1446±636	1062±214
Leukocyte rolling flux fraction	0.20±0.24	0.21±0.12	0.07±0.03†
Leukocyte adherence, mm^{-1}	203±224	1195±690*	750±384*

*$P<0.05$ vs wild-type.
†$P<0.05$ vs wild-type+TNF-α.

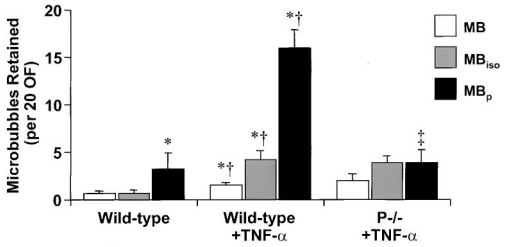

Figure 2. Mean±SEM number of microbubbles retained in 20 optical fields encompassing cremasteric venules of wild-type, TNF-α–treated wild-type, and TNF-α–treated $P^{-/-}$ mice. *$P<0.05$ vs other microbubbles in same cohort; †$P<0.05$ vs untreated wild-type data; ‡$P<0.01$ vs wild-type+TNF-α.

Examples of the different mechanisms for microbubble retention in a TNF-α–treated wild-type mouse are illustrated in Figure 4. Attachment of fluorescent MB_p microbubbles directly to the venular endothelium and to the surface of an activated leukocyte are shown in Figure 4A and 4B, respectively. Dual-fluorescence imaging in animals undergoing in vivo platelet labeling demonstrated occasional attachment of MB_p to the platelet components of leukocyte-platelet complexes adherent to the venular endothelium (Figure 4C and 4D). This phenomenon was often responsible for classification of attachment as indeterminate (in proximity but not directly contiguous to a leukocyte).

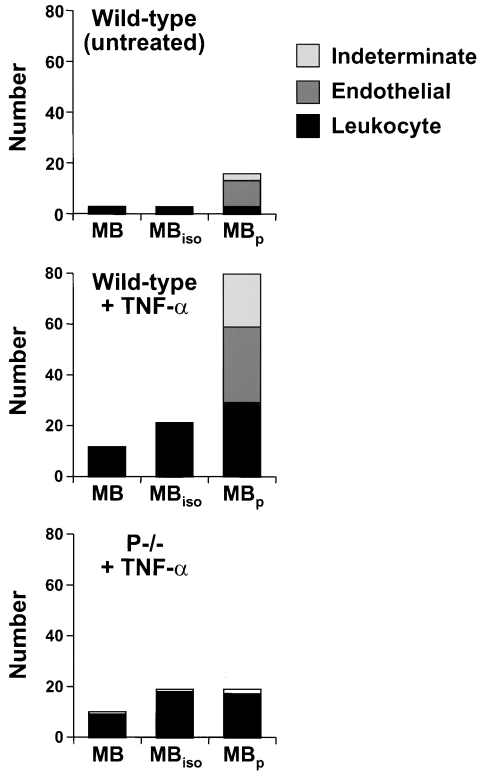

Figure 3. Mechanisms responsible for retention of microbubbles in cremasteric venules of wild-type, TNF-α–treated wild-type, and TNF-α–treated $P^{-/-}$ mice. Mechanisms were defined as attachment to leukocytes, attachment to endothelium, or indeterminate. Frequency of endothelial or indeterminate attachment was greater ($P<0.05$) for MB_p than MB or MB_{iso} in wild-type and TNF-α–treated wild-type animals.

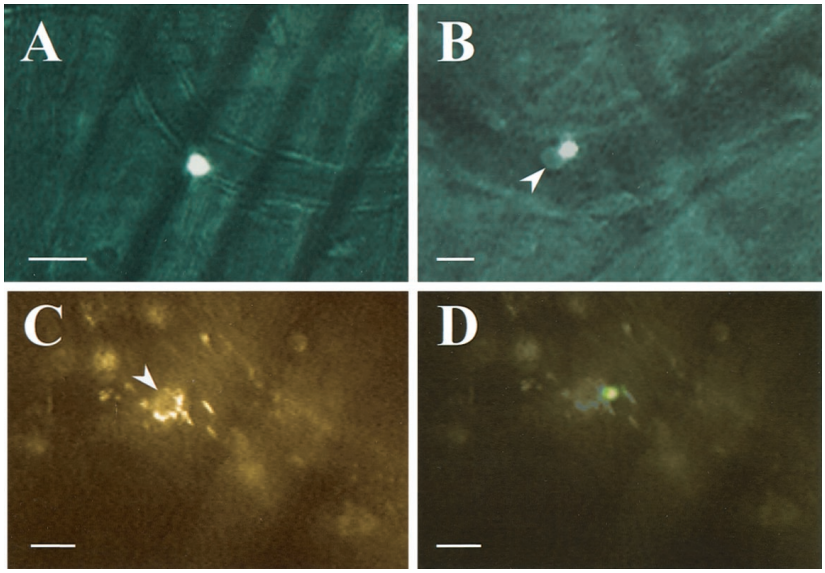

Figure 4. Intravital microscopy images illustrating mechanisms for microbubble retention in a TNF-α–treated wild-type mouse. Fluorescent MB_p microbubbles are shown binding (A) directly to the venular endothelium and (B) to an activated adherent leukocyte (arrow). In animals treated with rhodamine-6G, platelet-leukocyte complexes (C) were observed on the endothelial surface (arrow denotes leukocyte). In the same field, composite image for dual fluorescent imaging (D) demonstrates a microbubble attached to the complex via platelet binding. Bar=10 μm.

Contrast-Enhanced Ultrasound Imaging of Inflammation

Examples of contrast-enhanced renal ultrasound images after ischemia-reperfusion are illustrated in Figure 5. Contrast enhancement in the initial images obtained 8 minutes after injection reflects both retained and freely circulating microbubbles.[2] This signal was much greater for MB_p than MB in the wild-type animal undergoing ischemia-reperfusion, whereas signal from MB_p was low in the $P^{-/-}$ mouse. The signal in frames subsequently obtained at a PI of 10 seconds was uniformly very low, indicating the near absence of freely circulating microbubbles.

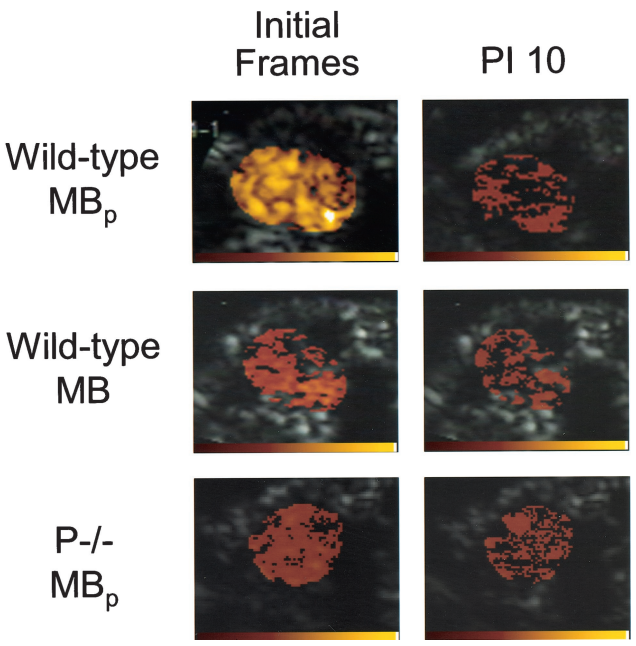

Figure 5. Background-subtracted color-coded ultrasound images of kidneys 1 hour after ischemia-reperfusion injury in wild-type and $P^{-/-}$ mice. Initial images acquired 8 minutes after intravenous injection of microbubbles and images subsequently obtained at PI of 10 seconds are shown. A 256-level color scale for background-subtracted VI is illustrated at bottom of each image.

The mean acoustic signal from retained microbubbles, calculated by subtracting the VI at a PI of 10 seconds from that on the initial frame,[2] was low in control kidneys for all microbubble agents (Figure 6). The signal from retained microbubbles increased for all microbubble agents after ischemia-reperfusion in wild-type mice but was significantly higher for MB_p than control microbubbles. Enhanced signal for MB_p compared with the other microbubbles in postischemic kidneys was abolished in $P^{-/-}$ mice. For control microbubbles, there was a trend toward lower signal in $P^{-/-}$ than in wild-type mice after ischemia-reperfusion.

Endothelial P-selectin expression in glomerular and peritubular vessels by immunohistology was greater in wild-type mice undergoing ischemia-reperfusion than in controls (Figure 7). P-selectin staining of intravascular platelet aggregates, especially in the outer medulla, was occasionally observed only in postischemic kidneys.

Discussion

We recently showed that lipid and albumin microbubbles are retained within the microcirculation of inflamed tissue because of their attachment to activated leukocytes[1–3] and can be detected by ultrasound imaging.[1,2] In the present study, we

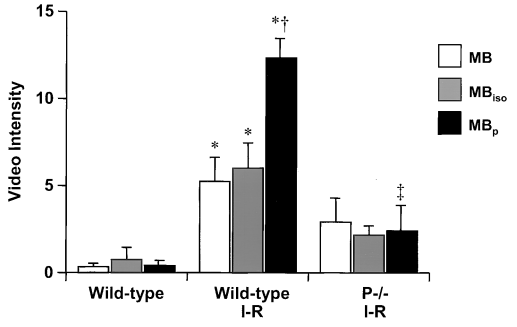

Figure 6. Mean±SEM background-subtracted VI from microbubbles retained within kidneys in control wild-type mice and after ischemia-reperfusion (I-R) in wild-type and $P^{-/-}$ mice. *$P<0.05$ vs control kidneys; †$P<0.01$ vs MB and MB_{iso}; ‡$P<0.01$ vs MB_p in wild-type I-R. OF indicates optical field.

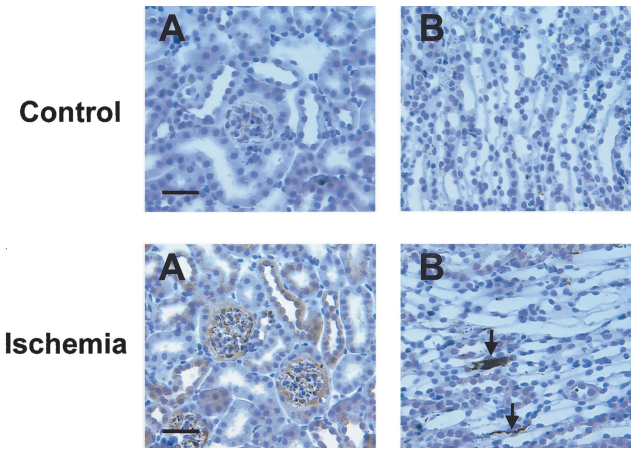

Figure 7. Immunohistochemistry of control and postischemic kidneys in wild-type mice. In postischemic kidneys, P-selectin expression in glomerular and peritubular vessels (A) was greater. In the outer medulla (B), large vascular platelet aggregates (arrows) were seen only in postischemic kidneys. Bar=50 μm.

demonstrate that targeting microbubbles to P-selectin greatly increases their retention by the mechanisms depicted in Figure 8 and enhances their ultrasound signal within injured tissue. These results suggest that ligand-targeted microbubbles may provide a reliable method for assessing the extent and degree of inflammation and tissue injury noninvasively with ultrasound.

Accumulation of leukocytes in regions of inflammation relies on a sequence of events characterized by leukocyte capture and rolling along the venular endothelium, progressive activation of rolling leukocytes, firm adhesion, and finally transmigration through the vessel wall.[16] The initial process of leukocyte rolling is mediated primarily by the selectin family of adhesion molecules.[16,17] In the present study, we targeted microbubbles against P-selectin by conjugating monoclonal antibodies against murine P-selectin to the surface of lipid-shelled microbubbles via a biotin-streptavidin system.

Retention of P-selectin–targeted microbubbles in inflamed tissue was evaluated by direct microscopic observation of their behavior in the cremasteric microcirculation of mice and by detection of microbubble signal after renal injury. For intravital microscopy experiments, untreated wild-type animals were used to evaluate microbubble behavior at baseline.

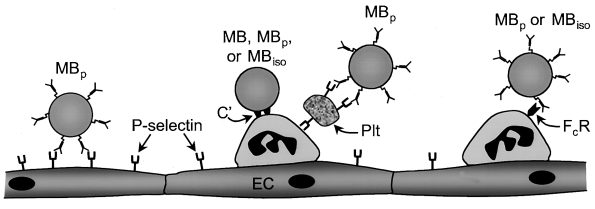

Figure 8. Mechanisms of microbubble retention. Nontargeted and probably targeted phospholipid microbubbles bind to adherent leukocytes through complement (C').[3] Microbubbles conjugated with antibody (MB$_p$ or MB$_{iso}$) show slightly enhanced binding, most likely due to interactions with immunoglobulin receptors on leukocytes (FcR). Only microbubbles conjugated with mAb RB40.34 against P-selectin (MB$_p$) also bind to P-selectin on endothelial cells (EC) or platelets (Plt).

These observations, however, do not represent true negative controls, because trauma induced by surgical exteriorization of the cremaster muscle resulted in rapid leukocyte rolling. Early rolling in this setting is almost entirely dependent on recruitment of P-selectin to the surface of venular endothelial cells from preformed stores within Weibel-Palade bodies.[12,17] Accordingly, a small degree of attachment of MB$_p$ directly to the venular endothelium was observed in untreated wild-type animals. There was also infrequent attachment for all 3 agents to the few leukocytes adherent in regions of more severe surgical trauma. For ultrasound experiments, true negative controls were available, because nonischemic kidneys were not instrumented. As a result, there was essentially no ultrasound signal from retained microbubbles in control kidneys during ultrasound imaging.

More intense inflammation in the cremaster muscle was produced by cytokine stimulation with TNF-α. Cytokine stimulation of the cremaster muscles resulted in a marked increase in venular leukocyte adherence. Consequently, the extent of microbubble attachment to leukocytes increased. The degree of leukocyte retention was slightly greater for microbubbles that contained antibodies (either control or P-selectin–specific antibody), most likely because of enhanced opsonization or interaction with immunoglobulin receptors expressed by leukocytes.[18] Leukocyte recruitment in the cremasteric microcirculation after treatment with TNF-α is promoted by increased venular endothelial expression of P-selectin.[19] Hence, retention of MB$_p$ was much greater than for either of the control microbubbles, largely because of a population that attached directly to the venular endothelial surface.

Early inflammatory responses after ischemia-reperfusion of the heart and kidney are supported by marked luminal expression of P-selectin.[20,21] For ultrasound imaging studies, a model of renal ischemic injury was used that results in P-selectin expression within 1 hour of reperfusion.[20,22] In accordance with our intravital microscopy experiments, the ultrasound signal from retained microbubbles in postischemic kidneys was greater for MB$_p$ than for control microbubbles. Renal immunohistology showed endothelial P-selectin expression, suggesting that binding to P-selectin was at least partially responsible for enhanced retention of targeted microbubbles.

To determine whether enhanced retention of MB$_p$ microbubbles was specifically due to P-selectin binding, microbubble behavior in the cremasteric microcirculation was assessed in TNF-α–stimulated P$^{-/-}$ mice. Direct attachment of MB$_p$ to the endothelium was completely abolished in these mice. Consequently, the extent of retention for MB$_p$ was similar to that found for microbubbles containing isotype control antibody and was mediated solely by attachment to leukocytes (cytokine-stimulated leukocyte adhesion still occurs in P$^{-/-}$ mice because of other adhesion pathways).[12,23] Similarly, contrast-enhanced ultrasound of postischemic kidneys in P$^{-/-}$ mice did not demonstrate greater signal for MB$_p$ than control microbubbles. In P$^{-/-}$ mice, leukocyte recruitment into tissue after renal ischemia-reperfusion is blunted,[13] which probably explains the lower signal obtained in postischemic kidneys in P$^{-/-}$ than wild-type mice for the control microbubbles.

Activated platelets also express P-selectin, which can mediate their attachment to activated leukocytes after ischemia-reperfusion injury.[24] We investigated whether platelet bridging between microbubbles and leukocytes could at least partially account for MB_p retention that occurred by an "indeterminate" mechanism in TNF-α–treated wild-type mice. In vivo fluorescent labeling of platelets confirmed attachment of MB_p microbubbles to platelet-leukocyte aggregates adherent to the venular endothelium, whereas attachment to platelets that transiently adhered directly to the endothelium was not seen. In the renal ischemia-reperfusion model, immunohistology suggested that cellular aggregates containing platelets may also have contributed to higher signal intensity for retained MB_p microbubbles.

The rationale for developing microbubbles targeted against P-selectin was to increase microbubble retention within the microcirculation, and hence, signal on ultrasound imaging of inflamed tissue. Although other acoustically active contrast agents with antibodies against intercellular adhesion molecule-1 conjugated to their surface have been developed,[4,25] the clinical feasibility of imaging with these agents has not been demonstrated. Our results indicate that ultrasound imaging of targeted microbubbles may provide a means to noninvasively assess inflammation and tissue injury. It must be acknowledged that tissue accumulation of microbubbles directed toward a molecular target is also likely to be influenced by other physiological parameters, such as regional perfusion. Therefore, further investigation into how microbubble retention is influenced by tissue hyperemia or postischemic microvascular "no-reflow" is warranted. Varying rates of clearance from the vascular pool for different microbubble agents, depending on their composition, may also affect the extent of microbubble retention by limiting or enhancing their recirculation through the target organ.

The results of this study imply that contrast ultrasound with targeted microbubbles not only may be useful for assessing inflammation but also could potentially be used to image other endothelial phenotypes (such as angiogenesis, tumor formation, and metastasis). Moreover, recent reports of enhanced gene transfer[26,27] in vivo by use of acoustic disruption of microbubbles suggest that the potential applications of targeted microbubbles may extend beyond diagnostic studies and into the realm of therapeutics by site-specific delivery of drugs or genes.

Acknowledgments

This study was supported in part by grants (HL-03810 [Dr Lindner] and HL-64381 [Dr Ley]) from the National Institutes of Health, Bethesda, Md, and by a Beginning Grant-in-Aid (Dr Lindner) and Fellowship Training Grant (Dr Christiansen) from the American Heart Association, Mid-Atlantic Affiliate, Baltimore, Md. The authors are grateful to Sanjiv Kaul, MD, for his review of the manuscript and to Mark Okusa, MD, and John Sanders, BS, for their assistance with immunohistology.

References

1. Lindner JR, Dayton PA, Coggins MP, et al. Noninvasive imaging of inflammation by ultrasound detection of phagocytosed microbubbles. *Circulation*. 2000;102:531–538.
2. Lindner JR, Song J, Xu F, et al. Noninvasive ultrasound imaging of inflammation using microbubbles targeted to activated leukocytes. *Circulation*. 2000;102:2745–2750.
3. Lindner JR, Coggins MP, Kaul S, et al. Microbubble persistence in the microcirculation during ischemia-reperfusion and inflammation: integrin- and complement-mediated adherence to activated leukocytes. *Circulation*. 2000;101:668–675.
4. Villanueva FS, Jankowski RJ, Klibanov S, et al. Microbubbles targeted to intercellular adhesion molecule-1 bind to activated coronary artery endothelial cells. *Circulation*. 1998;98:1–5.
5. Bevilacqua MP, Nelson RM. Selectins. *J Clin Invest*. 1993;91:379–387.
6. Kanwar S, Smith CW, Kubes P. An absolute requirement for P-selectin in ischemia/reperfusion-induced leukocyte recruitment in cremaster muscle. *Microcirculation*. 1998;5:281–287.
7. Klibanov AL, Gu H, Wojdyla JK, et al. Attachment of ligands to gas-filled microbubbles via PEG spacer and lipid residues anchored at the interface. *Proceedings of the 26th International Symposium on Controlled Release of Bioactive Materials*. 1999:124–125.
8. Bullard DC, Qin L, Lorenzo I, et al. P-selectin/ICAM-1 double mutant mice: acute emigration of neutrophils into the peritoneum is completely absent but is normal into pulmonary alveoli. *J Clin Invest*. 1995;95:1782–1788.
9. Lehr J, Vollmar B, Vajkoczy P, et al. Intravital fluorescence microscopy for the study of leukocyte interactions with platelets and endothelial cells. *Methods Enzymol*. 1999;300:462–481.
10. Lipowski HH, Zweifach BW. Application of the "two-slit" photometric technique to the measurement of microvascular volumetric flow rates. *Microvasc Res*. 1978;15:93–101.
11. Reneman RS, Woldhuis B, oude Egbrink MGA, et al. Concentration and velocity profiles of blood cells in the microcirculation. In: Hwang NHC, Turitto VT, Yen MRT, eds. *Advances in Cardiovascular Engineering*. New York, NY; Plenum; 1992:25–40.
12. Ley K, Bullard DC, Arbones ML, et al. Sequential contribution of L- and P-selectin to leukocyte rolling in vivo. *J Exp Med*. 1995;181:669–675.
13. Singbartl K, Green SA, Ley K. Blocking P-selectin protects from ischemia/reperfusion induced acute renal failure. *FASEB J*. 2000;14:48–54.
14. Wei K, Jayaweera AR, Firoozan S, et al. Quantification of myocardial blood flow with ultrasound-induced destruction of microbubbles administered as a constant venous infusion. *Circulation*. 1998;97:473–483.
15. Green SA, Setiadi H, McEver RP, et al. The cytoplasmic domain of P-selectin contains a sorting determinant that mediates rapid degradation in lysosomes. *J Cell Biol*. 1994;124:435–448.
16. Springer T. Traffic signals on endothelium for lymphocyte recirculation and leukocyte emigration. *Annu Rev Physiol*. 1995;57:827–872.
17. Gaboury JP, Johnston B, Nieu XF, et al. Mechanisms underlying acute mast cell-induced leukocyte rolling and adhesion in vivo. *J Immunol*. 1995;154:804–813.
18. Heyman B. Regulation of antibody responses via antibodies, complement, and Fc receptors. *Annu Rev Immunol*. 2000;18:709–737.
19. Jung U, Ley K. Regulation of E-selectin, P-selectin, and intercellular adhesion molecule-I expression in mouse cremaster muscle vasculature. *Microcirculation*. 1997;4:311–319.
20. Zizzi HC, Zibari GB, Granger DN, et al. Quantification of P-selectin expression after renal ischemia and reperfusion. *J Pediatr Surg*. 1997;32:1010–1013.
21. Lefer DJ. Pharmacology of selectin inhibitors in ischemia/reperfusion states. *Annu Rev Pharmacol Toxicol*. 2000;40:283–294.
22. Okusa MD, Linden J, Huang L, et al. A_2 adenosine receptor mediated inhibition of ischemia reperfusion injury and neutrophil adhesion in rat and mouse kidneys. *Am J Physiol*. 2000;279:F809–F818.
23. Jung U, Ramos CL, Bullard DC, et al. Gene-targeted mice reveal importance of L-selectin-dependent rolling for neutrophil adhesion. *Am J Physiol*. 1998;274:H1785–H1791.
24. Weyrich AS, Ma XI, Lefer DJ, et al. In vivo neutralization of P-selectin protects feline heart and endothelium in myocardial ischemia and reperfusion injury. *J Clin Invest*. 1993;88:1396–1406.
25. Demos SM, Alkan-Onyuksel H, Kane BJ, et al. In vivo targeting of acoustically active reflective liposomes for intravascular and transvascular ultrasonic enhancement. *J Am Coll Cardiol*. 1999;33:867–875.
26. Shohet RV, Chen S, Zhou Y, et al. Echocardiographic destruction of albumin microbubbles directs gene delivery to the myocardium. *Circulation*. 2000;101:2554–2556.
27. Porter TR, Iversen PL, Li S, et al. Interaction of diagnostic ultrasound with synthetic oligonucleotide-labeled perfluorocarbon-exposed sonicated dextrose albumin microbubbles. *J Ultrasound Med*. 1996;15:577–584.